



Antimicrobial peptide Cathelicidin-BF prevents intestinal barrier dysfunction in a mouse model of endotoxemia



Deguang Song, Xin Zong, Haiwen Zhang, Tenghao Wang, Hongbo Yi, Chao Luan, Yizhen Wang*

National Engineering Laboratory of Biological Feed Safety and Pollution Prevention and Control, Key laboratory of Molecular Animal Nutrition, Ministry of Education, Institute of Feed Science, Zhejiang University, Hangzhou, China

ARTICLE INFO

Article history:

Received 23 November 2014
Received in revised form 15 January 2015
Accepted 20 January 2015
Available online 29 January 2015

Keywords:

Antimicrobial peptide
Intestinal permeability
Tight junction
Apoptosis
NF- κ B

ABSTRACT

Intestinal barrier functions are altered during the development of sepsis. Cathelicidin antimicrobial peptides, such as LL-37 and mCRAMP, can protect animals against intestinal barrier dysfunction. Cathelicidin-BF (C-BF), a new cathelicidin peptide purified from the venom of the snake *Bungarus fasciatus*, has been shown to have both antimicrobial and anti-inflammatory properties. This study investigated whether C-BF pretreatment could protect the intestinal barrier against dysfunction in a mouse model of endotoxemia, induced by intraperitoneal injection of LPS (10 mg/kg). Mice were treated with low or high dose C-BF before treatment with LPS, and samples were collected 5 h after LPS treatment. C-BF reduced LPS induced intestinal histological damage and gut permeability to 4 KD Fluorescein–isothiocyanate-conjugated dextran. Pretreatment with C-BF prevented LPS induced intestinal tight junction disruption and epithelial cell apoptosis. Moreover, C-BF down regulated the expression and secretion of TNF- α , a process involving the NF- κ B signaling pathway. C-BF also reduced LPS induced TNF- α expression through the NF- κ B signaling pathway in mouse RAW 264.7 macrophages. These findings indicate that C-BF can prevent gut barrier dysfunction induced by LPS, suggesting that C-BF may be used to develop a prophylactic agent for intestinal injury in endotoxemia.

© 2015 Elsevier B.V. All rights reserved.

1. Introduction

Endotoxemia can induce sepsis, one of the leading causes of death in noncardiac intensive care units worldwide [1]. Derangements in intestinal function are crucial in the development of sepsis [2], indicating that the gut functions as the “motor” of systemic inflammatory responses [3]. Intestinal barrier function depends primarily on the integrity of the intestinal epithelium, which is responsible for restricting the translocation of harmful agents, such as microorganisms and toxins via both transcellular and paracellular pathways [4]. The integrity of the intestinal epithelium requires a delicate balance between epithelial cell proliferation and death [5,6], and the regulation of TJ proteins [7]. Systemic inflammation such as sepsis has been shown to accelerate IEC apoptosis and shedding [8], and to disrupt TJ proteins [9], processes driven by NF- κ B dependent TNF- α expression [10] and myosin light chain (MLC) kinase activation [11], resulting in subsequent gut barrier dysfunction.

Abbreviations: LPS, Lipopolysaccharide; FD4, 4 KD Fluorescein–isothiocyanate-conjugated dextran; TJ, Tight junction; DSS, Dextran sulfate sodium; PBS, phosphate-buffered saline; TNF- α , tumor necrosis factor- α ; IEC, intestinal epithelial cell.

* Corresponding author at: Institute of Feed Science, Zhejiang University, 866 Yuhangtang Road, Hangzhou 310058, China. Tel.: +86 571 88982815; fax: +86 571 88982650.

E-mail address: yzwang@zju.edu.cn (Y. Wang).

Cathelicidins, a family of antimicrobial peptides with anti-bacterial, anti-viral, and anti-fungal properties [12], act as multifunctional effector molecules in innate immunity [13]. In humans, LL-37 is the major cathelicidin peptide derived from the gene CAMP, whereas in mice the homologous peptide mCRAMP serves similar functions as the human LL-37 [14]. LL-37 is anti-endotoxic protein, which selectively inhibits pro-inflammatory cytokine production in response to LPS [15,16], and shows protective activity in a mouse model of endotoxemia [17]. Moreover, cathelicidin expression was found to be altered in patients with ulcerative colitis (UC) [18]. Endogenous cathelicidin can modulate colon tissue apoptosis during DSS-induced intestinal inflammation in cathelicidin mCRAMP-deficient mice [19]. Moreover, intrarectal administration of mCRAMP could prevent colitis development by suppressing apoptosis induction and neutrophil infiltration [20].

C-BF, a cathelicidin-like antimicrobial peptide purified from the venom of the snake *Bungarus fasciatus*, consists of 30 amino acids. Its secondary structure is an amphipathic α -helical conformation. It has been shown to kill several microorganisms more efficiently than LL-37 and clindamycin do [21]. Moreover, C-BF is stable in mouse plasma for at least 2.5 h [22] and can relieve *Propionibacterium acnes*-induced mouse ear swelling and granulomatous inflammation [21]. This study was designed to investigate whether C-BF can prevent LPS induced intestinal barrier dysfunction.

2. Materials and methods

2.1. Peptide synthesis

C-BF (KFFRKLKKSVKKRAKEFFKKPRVIGVSIPF) were synthesized by standard solid-phase procedures with 9-fluorenylmethoxycarbonyl (Fmoc) approach using an Apex 396 peptide synthesizer (Aapptec, Louisville, KY, USA) by GL Biochem (Shanghai, China) Ltd. Ninety-five percent purity of C-BF was achieved, verified by using Agilent 1200 Series high-performance liquid chromatography (Agilent technologies, CA, USA) and Thermo Finnigan LCQ ion trap mass spectrometer (Thermo Finnigan, San Jose, CA, USA). The peptide was dissolved in sterile saline at the concentration of 1 mg/ml (for high dose treatment) and 0.5 mg/ml (for low dose treatment), and stored at -80°C until use.

2.2. Reagents

LPS from the Escherichia coli serotype 0111:B4 was purchased from Sigma-Aldrich, and was dissolved in sterile saline at the concentration of 1.25 mg/ml. FD4 was purchased from Sigma-Aldrich. The rabbit antibodies for β -actin and occludin were purchased from Abcam (Cambridge, UK). The rabbit antibodies for ZO-1, NF- κ B p65 and phospho p-65 were purchased from Santa Cruz Biotechnology (Santa Cruz, CA, USA). The secondary antibody goat-anti-rabbit IgG was purchased from Boster (Wuhan, China).

2.3. Animals

Male ICR mice (22–27 g) were obtained from Laboratory Animal Services Centre of the Zhejiang University. All animals were housed individually in plastic cages with standard chow diet and water and allowed to acclimate to their environment for 1 week before the experiment. The animal experimental protocols were approved by the Animal Care and Use Committee of Zhejiang University.

2.4. Treatment groups and medication procedure

All the mice had free access to water and food throughout the experiment. The mice were randomly divided into 6 groups of 10 each: control (control), low dose (4 mg/kg) C-BF-treated (LC-BF), high dose (8 mg/kg) C-BF-treated (HC-BF), LPS-treated (LPS), low dose C-BF pretreated followed by LPS treated (LC-BF + LPS) and high dose C-BF pretreated followed by LPS treated (HC-BF + LPS) mice. These dosages were chosen on the basis of our unpublished data that 2 mg/kg–10 mg/kg C-BF were more effective in ameliorating inflammation response. C-BF (200 μ l each mouse) was injected intraperitoneally once per day for 6 days, whereas the control and LPS groups were intraperitoneally injected with an equal volume of sterile saline. On day 6, mice in the LPS, LC-BF + LPS and HC-BF + LPS groups were intraperitoneally injected with received LPS (10 mg/kg, 200 μ l each mouse) 1 h after C-BF or saline treatment; the other groups were injected with an equal volume of saline. None of the mice died during the experiment. All mice were killed 5 h after intraperitoneal injection of LPS or saline.

2.5. Measurement of serum TNF- α

The serum levels of TNF- α were determined using an ELISA kit (Multisciences, Hangzhou, China) according to the manufacturer's protocol.

2.6. Histopathological evaluation

Images of paraffin section of duodenum, jejunum, and ileum were obtained using a Leica DM3000 Microsystem (Leica, Wetzlar, Germany) with Leica Application Suite Version 3.7.0. The villi height and crypt depth were measured by using the ImageJ [23] segmented

line tool. 3 pathologists, blinded to the source of the slides, analyzed and reported on each slide of jejunum. The degree of histopathologic changes was graded by using the histologic injury scale described by Chiu et al. [24] (Table 1).

2.7. Gut permeability assessment

FD4 was administered at 20 ml/kg body weight by oral gavage 1 h after LPS or saline administration. Serum fluorescence was measured by a Molecular Devices SpectraMax M5 plate reader (excitation 485 nm, emission 535 nm).

The 40 mg/ml FD4 was diluted with 5120, 2560, 1280, 640, 320, 160, 80, 40, 20, 10, and 5 ng/ml with PBS as the standard curve, and calculated the serum FD4 concentration through the standard curve.

2.8. Western blot analysis

Total protein extracts of jejunum were prepared by a Total Protein Extraction Kit (KeyGen BioTECH, Nanjing, China) according to the manufacturer's protocol. Lysates protein concentration were quantified by a BCA Protein Quantification Kit (KeyGen BioTECH, Nanjing, China). Equivalent amounts of protein were subjected to SDS-PAGE and electro blotted onto PVDF membranes (Millipore, Billerica, MA, USA). The membranes were incubated overnight at 4°C with the following primary antibodies: β -actin, ZO-1, occludin, NF- κ B p65, and phospho-NF- κ B p65. Then membranes were incubated with anti-rabbit IgG antibodies for 1 h.

2.9. RNA extraction and real-time PCR

Total RNA was isolated using the TRIzol reagent (Invitrogen Life Technology), and the RNA concentration was quantified by the NanoDrop ND-1000 spectrophotometer (Thermo Scientific, Waltham, MA, USA). Total RNA was subjected to reverse transcription (RT) reaction with random primers. Quantitative PCR was performed by StepOne Plus™ Real Time PCR System (Applied Biosystems, Foster City, CA, USA) using a Faststart Universal SYBR Green Master (ROX) (Roche Diagnostics, Mannheim, Germany). The gene-specific primers were designed using Primer Premier 5.0 (Table 2).

2.10. Immunohistochemistry for apoptotic IECs

The apoptotic IECs were identified by TUNEL (in situ cell death detection kit, KeyGen BioTECH, Nanjing, China). Labeled cells were analyzed by a Leica DM3000 microsystem. The number of apoptotic cells and the total cell number per field in each slide were counted. A minimum of 500 cells and 5 high-powered fields were counted per slides. The apoptosis index (AI) was calculated according to the following formula:

$$\text{AI} = \frac{\text{the number of apoptotic cells (AC)}}{\text{the number of intact cells (IC)}} \times 100$$

Table 1
Intestinal mucosal damage grading score.

Grade	Histological characteristic(s)
Grade 0	Normal mucosal villi
Grade 1	Subepithelial Gruenha gen's space (oedema), usually at the apex of the villus
Grade 2	Extension of the subepithelial space with moderate lifting of epithelial layer from the lamina propria
Grade 3	Massive epithelial lifting down the sides of villi; a few tips may be denuded
Grade 4	Denuded villi with lamina propria and dilated capillaries exposed
Grade 5	Digestion and disintegration of lamina propria; hemorrhage and ulceration

Table 2

PCR primer sequence used in this study and their Tm values.

Primer	Sequence (5'–3')	Tm (°C)
TNF-α forward	GCATGGTGGTGGTTGTTTCTGACGAT	60
TNF-α reverse	GCTTCTGTTGGACACCTGGAGACA	
ZO-1 forward	TCATCCCAAATAAGAACAGAGC	60
ZO-1 reverse	GAAGAACACCTTTTCATAAGC	
Occludin forward	CTTTGGCTACGGAGGTGGCTAT	60
Occludin reverse	CTTTGGCTGCTCTTGGGTCTG	
GAPDH forward	CAACGGCACAGTCAAGGCTGAGA	60
GAPDH reverse	CTCAGCACAGCATCACCCAT	

2.11. Cell culture and treatments

The mouse macrophage cell line RAW264.7 was obtained from the Institute of Biochemistry and Cell Biology, SIBS, CAS (Shanghai, China).

The cells were cultured in RPMI 1640 medium supplemented with 10% FBS, 100 U/ml of penicillin, 100 µg/ml of streptomycin at 37 °C with 5% CO₂ in a humidified atmosphere. Cells of the C-BF and C-BF + LPS groups were pretreated with 10 µg/ml C-BF, and the control and LPS groups were treated with same volume of PBS. After 6 h incubation, these cells were washed with D-Hanks and incubated in RPMI medium with PBS (control and C-BF groups), 1 µg/ml LPS (LPS and C-BF + LPS groups) for 2 h respectively.

2.12. Data analysis

All statistical calculations were carried out by SPSS 19.0. Data represent mean ± s.e.m. Significant differences between the control and experimental groups were determined by a one-way ANOVA with a Duncan multiple range test at *P* < 0.05. ^{abc}Bars with different small capital letters are statistically different from one another.

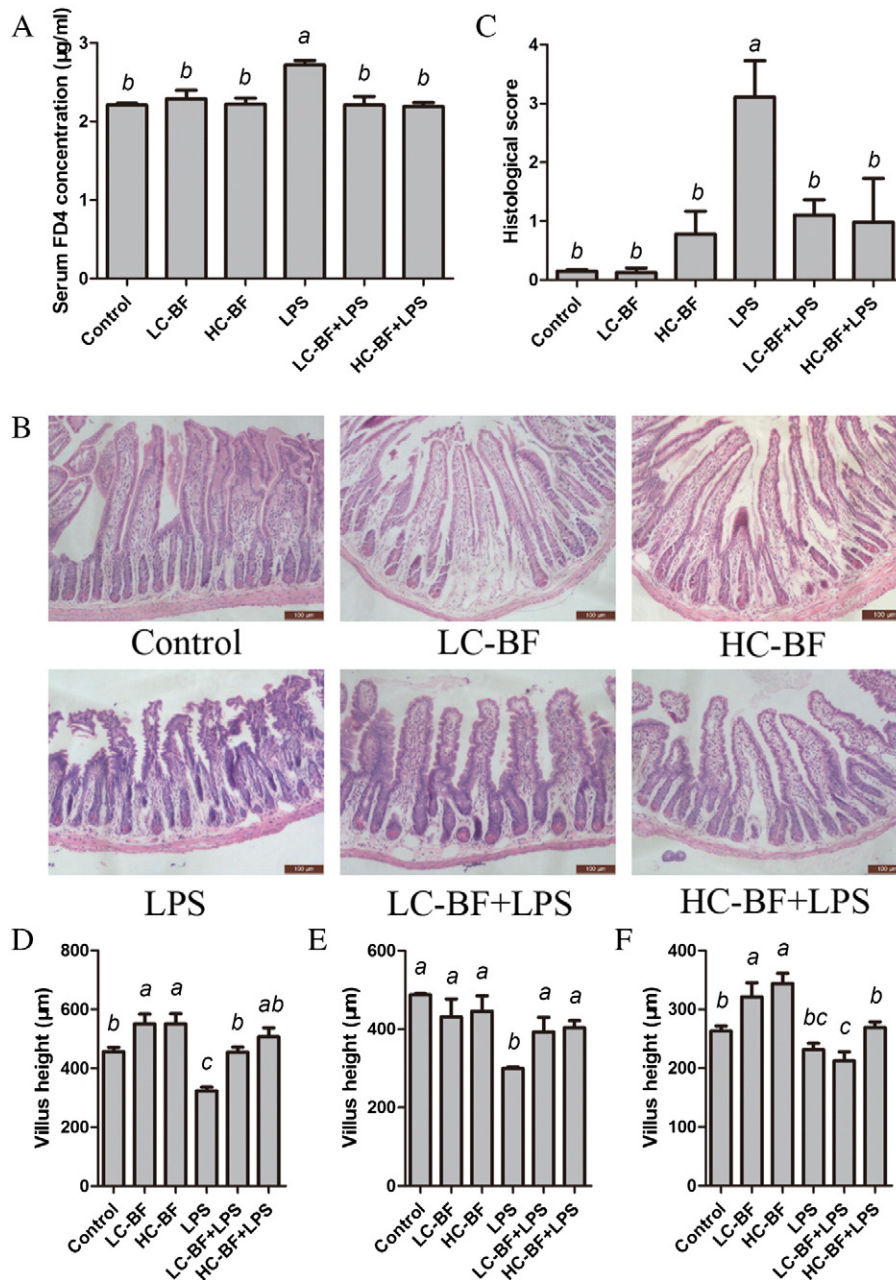


Fig. 1. Effect of C-BF on intestinal permeability, histological appearance, histological score of the jejunum and villus height in the duodenum, jejunum and ileum. (A) Intestinal permeability. (B) Photomicrographs of sections of jejunal samples (×100). (C) Mucosal damage grading. Villus heights of the duodenum (D), jejunum (E) and ileum (F).

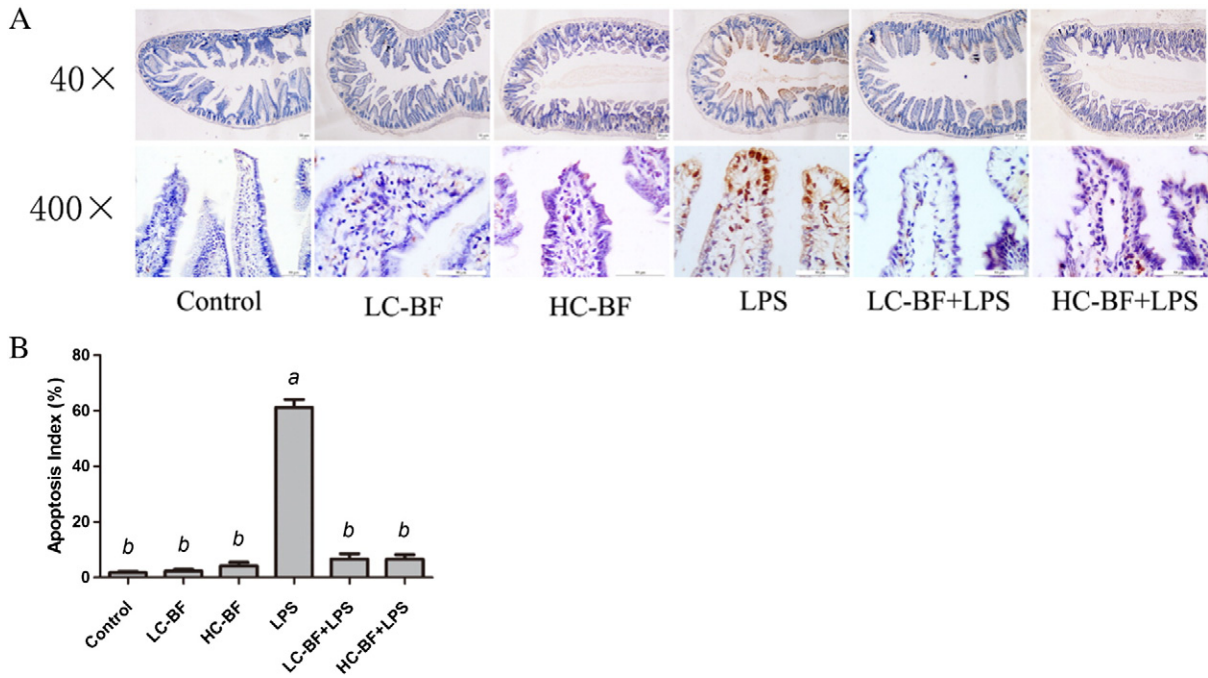


Fig. 2. Effect of C-BF on small intestinal cell apoptosis. (A) Representative TUNEL images for cell apoptosis (browen signals, original magnification 40×, 400×). (B) Apoptosis index of jejunal tissues.

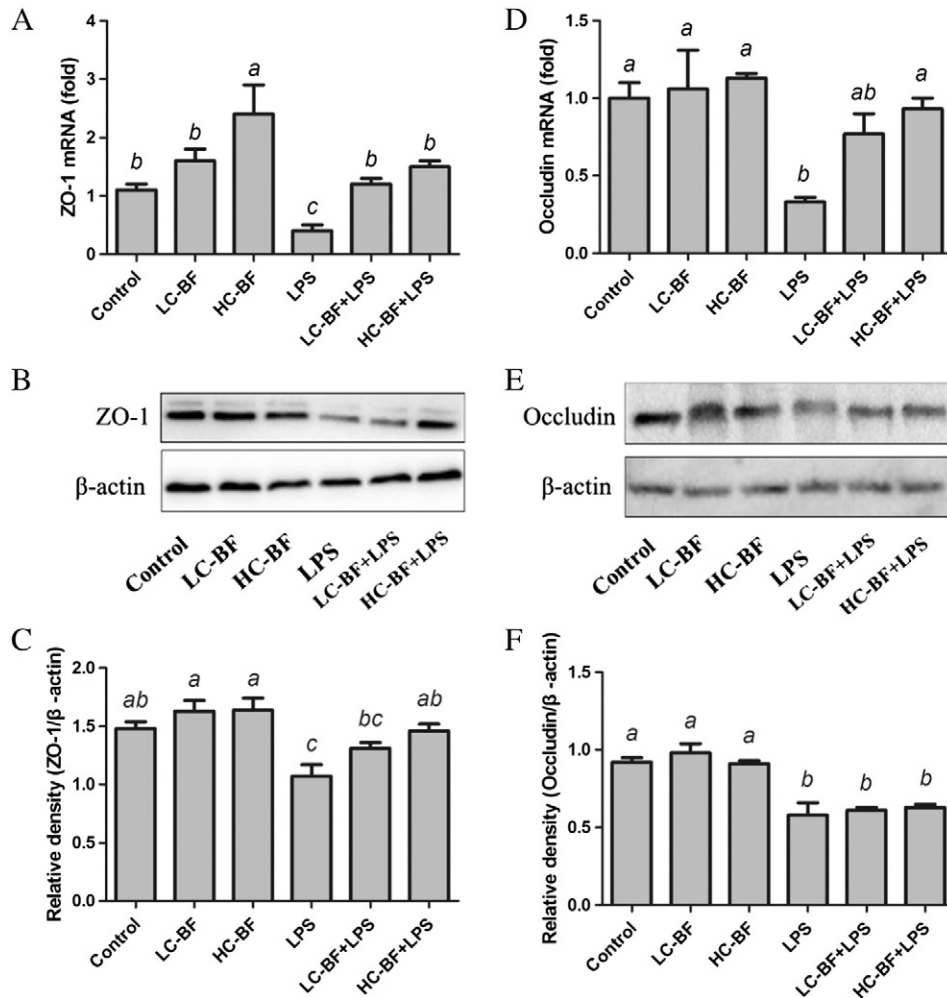


Fig. 3. Effect of C-BF on jejunal epithelial tight junction expression. (A and D) Real time PCR analysis of ZO-1 (A) and occludin (D) mRNA abundance in jejunum. (B, C and E, F) Western blot analysis of the expression of ZO-1 (B and C) and occludin (E and F) protein in jejunum.

3. Results

3.1. Gut-to-circulation permeability

Six hours after LPS administration, serum FD4 concentration was significantly higher in LPS- than in untreated mice ($2.72 \pm 0.06 \mu\text{g/ml}$

vs $2.21 \pm 0.02 \mu\text{g/ml}$, $P < 0.05$; Fig. 1A). However, pretreatment with both 4 mg/kg and 8 mg/kg C-BF significantly reduced serum FD4 concentrations, to $2.11 \pm 0.11 \mu\text{g/ml}$ and $2.19 \pm 0.05 \mu\text{g/ml}$, respectively, compared with the LPS group ($P < 0.05$ each), which showed no marked difference from the control group. Moreover, C-BF alone did not significantly affect intestinal permeability, compared with the control group.

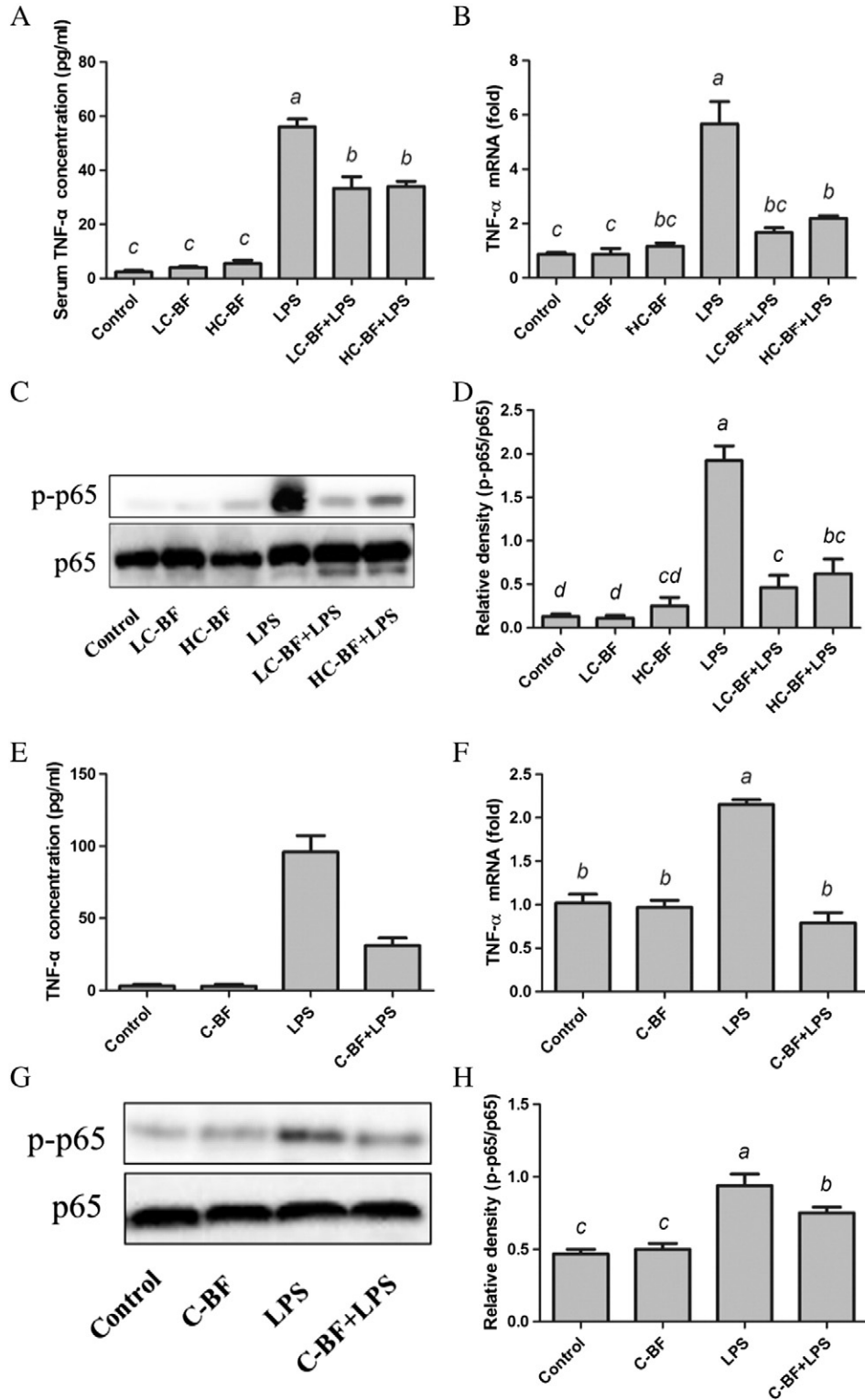


Fig. 4. Effect of C-BF on serum TNF-α concentration and TNF-α expression and NF-κB activation in jejunum and RAW 264.7 macrophages. (A) Serum TNF-α concentration. (B) Real time PCR analysis of TNF-α mRNA abundance in jejunum. (C and D) Western blot analysis of NF-κB phosphorylation in jejunum. (E) TNF-α concentration in the supernatant. (F) Real time PCR analysis of TNF-α mRNA abundance. (G and H) Western blot analysis of p65 phosphorylation induced by LPS.

3.2. Gross morphological and histopathological evaluations

H&E staining of specimens from the jejunums of control and C-BF (including LC-BF and HC-BF) treated mice showed integrated villi and compactly arrayed epithelium (Fig. 1B). In contrast, the intestines of LPS treated mice showed marked atrophy and blunting of the villi, with discontinuous brush borders and disarrayed epithelium. Pretreatment with C-BF followed by treatment with LPS resulted in minimal changes in the villi, similar to the control group. Based on mucosal damage score, C-BF pretreatment prevented intestinal mucosal damage induced by LPS (Fig. 1C).

Villus shortening is a frequently used measure of small intestinal damage. In the jejunum, mean villus heights of the LPS group were reduced 39% compared with the control group ($299.89 \pm 3.31 \mu\text{m}$ vs. $487.37 \pm 2.67 \mu\text{m}$; $P < 0.05$; Fig. 1E). Although C-BF did not alter villus heights, both doses significantly alleviated LPS induced villus shortening ($P < 0.05$ each), similar to those of control mice.

In the duodenum (Fig. 1D), C-BF pretreatment significantly alleviated villus shortening due to LPS, with a similar level to untreated mice. Additionally, mice treated with LC-BF and HC-BF in the absence of LPS showed significant greater villus heights than control group. In the ileum, however, LPS had no effect on villus height (Fig. 1F). Moreover, neither C-BF nor LPS treatments significantly altered crypt depth in the duodenum, jejunum and ileum (data not shown).

3.3. Intestinal epithelial cell apoptosis

Results from TUNEL analysis indicated that LPS treatment resulted in the apoptosis of jejunal epithelial cells (brown signals, Fig. 2A), which was quantified by measuring the apoptosis index (Fig. 2B). Pretreatment of LPS-administered mice with 4 mg/kg and 8 mg/kg C-BF significantly reduced the apoptosis index by 89.29% and 89.40% ($P < 0.05$ each), respectively. These indexes were comparable to that of the control group. Moreover, the apoptosis indexes in mice of LC-BF and HC-BF (without LPS) were similar to that in the control group.

3.4. Intestinal TJs expression

LPS reduced the expression of both ZO-1 mRNA and protein, by 64% and 27%, respectively, compared with the control group ($P < 0.05$ each; Fig. 3A–C). However, C-BF pretreatment completely and significantly abrogated the LPS-induced reduction in ZO-1 mRNA ($P < 0.05$) and the higher dose of C-BF significantly abrogated the LPS induced reduction in ZO-1 protein ($P < 0.05$). C-BF had similar effects on occludin mRNA expression, but its effects on occludin protein were not statistically significant (Fig. 3D–E).

3.5. Serum TNF- α level, intestinal TNF- α mRNA expression and NF- κ B activation

LPS treatment resulted in a 23-fold increase in serum TNF- α concentration compared with untreated mice ($56.02 \pm 2.94 \text{ pg/ml}$ vs. $2.43 \pm 0.67 \text{ pg/ml}$, $P < 0.05$; Fig. 4A). Pretreatment with 4 mg/kg and 8 mg/kg C-BF reduced LPS induced TNF- α secretion by 40.4% and 39.3%, respectively. Serum TNF- α concentration in mice treated with C-BF alone was similar to that of the control group.

Real time PCR analysis showed that LPS markedly enhanced TNF- α mRNA levels in jejunum compared with untreated mice (Fig. 4B), whereas, C-BF pretreatment significantly reduced TNF- α mRNA levels compared with LPS treated mice. In addition, TNF- α mRNA levels in mice of LC-BF and HC-BF groups, in the absence of LPS, were similar to that of control mice.

LPS stimulation also markedly activated p65, an activation significantly inhibited by C-BF pretreatment (Fig. 4C). Quantification showed that LPS increased the phospho-p65 signal 14.8 fold compared with

control mice ($P < 0.05$; Fig. 4D), whereas C-BF pretreatment significantly inhibited LPS induced p65 activation.

3.6. TNF- α expression in mouse RAW264.7 macrophages

Treatment of mouse RAW264.7 macrophages with LPS enhanced the concentration of TNF- α in the supernatant 36-fold compared with control mice, whereas C-BF pretreatment significantly reduced the secretion of TNF- α in response to LPS (Fig. 4E). A similar trend was also found in TNF- α mRNA expression. LPS induced a 2-fold increase in TNF- α mRNA expression, which was significantly inhibited by C-BF pretreatment (Fig. 4F). Western blot analysis indicated that C-BF significantly inhibited LPS mediated p65 activation. Additionally C-BF treatment, in the absence of LPS, did not significantly alter p65 activation, TNF- α mRNA abundance or TNF- α secretion compared with control group (Fig. 4G and H).

4. Discussion

This study suggested that the antimicrobial peptide C-BF may play an important role in the inhibition of LPS-mediated intestinal injury in endotoxemic mice. Intraperitoneal administration of C-BF significantly weakened LPS induced increases in permeability to large molecules and mucosal morphological damage. These effects of C-BF involved the inhibition of NF- κ B activation and TNF- α expression, leading to diminished mucosal apoptosis and TJ disruption. Thus, the intestine was able to maintain mucosal barrier function during endotoxemia.

The intestinal epithelial barrier is important in the systemic inflammatory response after LPS treatment. Barrier breakdown is characterized by typical histological changes and high gut permeability [25]. Acute systemic LPS administration was found to decrease villus height [10], induce morphological damage [25] and increase the movement of large molecules from the gut lumen to plasma [8]. Our model showed similar changes in villus height, histomorphology and gut-to-circulation permeability 5 h after LPS administration, but all of these effects were significantly inhibited by C-BF injection.

The gut barrier is composed of a single layer of IECs held together by TJs, with barrier loss in the intestine occurring at sites of excessive cell shedding [26]. LPS induced IEC apoptosis and cell shedding within 1.5 h in the small intestine, with IEC apoptosis occurring prior to shedding [10]. The results presented here show that LPS triggered severe cell apoptosis at apical villi, whereas C-BF pretreated mice showed strong resistance to LPS induced apoptosis and shedding.

TNF- α has been found to mediate LPS induced IEC apoptosis [10], and plasma TNF- α concentrations have been found to increase rapidly after LPS administration [27]. The findings presented here demonstrate that C-BF significantly inhibited LPS-induced increases not only of serum TNF- α , but of TNF- α mRNA abundance in the small intestine. The specific LPS receptor TLR4 has been found expressed at low levels in IECs [28], suggesting that the initial recognition of systemic LPS does not occur in IECs, but via TLR4 ligation in monocytes and macrophages, which in turn rapidly secrete cytokines, including TNF- α [29]. Assessments of the effects of C-BF on LPS treated RAW 264.7 macrophages showed that LPS significantly stimulated NF- κ B activation and TNF- α expression and secretion, all of which were significantly suppressed by C-BF. These findings suggest that C-BF inhibited NF- κ B activation and TNF- α expression and secretion in residue macrophages, significantly reducing IEC apoptosis.

The TJ proteins, such as ZO-1 and occludin, are important regulators of intestinal permeability. LPS was shown to reduce ZO-1 expression in nontumorigenic epithelial monolayers [30], to degrade gut occludin in rats [31] and significantly disrupting barrier function. Decreased ZO-1 protein expression has been found to correlate with increased paracellular permeability in endotoxemic animals [25]. Moreover, siRNA-induced knockdown of occludin in Caco-2 cells and mouse intestine was found to enhance the transepithelial flux of large molecules

such as dextran [32]. The results presented here showed that LPS down-regulated the expression of ZO-1 and occludin mRNA and protein, increasing intestinal permeability. However, C-BF pretreatment partially abrogated the effects of LPS on the expression of ZO-1 and occludin proteins and completely abolished the effects of LPS on ZO-1 and occluding mRNAs. In addition, C-BF was found to partially prevent the redistribution of ZO-1 and occludin induced by LPS in rats and IPEC-J2 cells (unpublished results).

LPS markedly stimulated the activation of NF- κ B. Activated NF- κ B p65 may bind to the myosin light-chain kinase (MLCK) promoter region and increase MLCK expression [33,34]. MLCK-mediated MLC phosphorylation has been found to result in the contraction of actin–myosin filaments, altering TJ protein localization and expression as well as TJ barrier functional openings [35]. The results presented here showed that C-BF markedly inhibited NF- κ B activation which may suppress the activation of MLCK and reduce the disruption of TJs. Therefore, the beneficial effects of C-BF on TJ may be partially mediated by the down-regulation of NF- κ B pathways.

In conclusion, this study has shown that C-BF can ameliorate intestinal mucosal apoptosis and epithelial TJ disruption in a mouse model of endotoxemia. The mechanism of action of C-BF may be associated with its inhibition of the NF- κ B signaling pathway. C-BF, alone or in combination with other agents, may serve as a potential new prophylactic agent to protect normal intestinal barrier function in patients with endotoxemia.

Acknowledgments

We gratefully acknowledge financial support from the National Natural Science Foundation for Distinguished Young Scholars of China (Grand No. 31025027) and the earmarked fund for Modern Agro-industry Technology Research System (CARS-36).

References

- [1] Angus DC, Linde-Zwirble WT, Lidicker J, Clermont G, Carcillo J, Pinsky MR. Epidemiology of severe sepsis in the United States: analysis of incidence, outcome, and associated costs of care. *Crit Care Med* 2001;29:1303–10.
- [2] Yu P, Martin CM. Increased gut permeability and bacterial translocation in *Pseudomonas pneumonia*-induced sepsis. *Crit Care Med* 2000;28:2573–7.
- [3] Hassoun HT, Kone BC, Mercer DW, Moody FG, Weisbrodt NW, Moore FA. Post-injury multiple organ failure: the role of the gut. *Shock* 2001;15:1–10.
- [4] Farhadi A, Banan A, Fields J, Keshavarzian A. Intestinal barrier: an interface between health and disease. *J Gastroenterol Hepatol* 2003;18:479–97.
- [5] Hall PA, Coates PJ, Ansari B, Hopwood D. Regulation of cell number in the mammalian gastrointestinal tract—the importance of apoptosis. *J Cell Sci* 1994;107:3569–77.
- [6] Watson AJM, Chu SY, Sieck L, Gerasimenko O, Bullen T, Campbell F, et al. Epithelial barrier function in vivo is sustained despite gaps in epithelial layers. *Gastroenterology* 2005;129:902–12.
- [7] Li QR, Zhang Q, Wang CY, Liu XX, Li N, Li JS. Disruption of tight junctions during polymicrobial sepsis in vivo. *J Pathol* 2009;218:210–21.
- [8] Lai CW, Sun TL, Lo W, Tang ZH, Wu S, Chang YJ, et al. Shedding-induced gap formation contributes to gut barrier dysfunction in endotoxemia. *J Trauma Acute Care* 2013;74:203–13.
- [9] Li HM, Wang YY, Wang HD, Cao WJ, Yu XH, Lu DX, et al. Berberine protects against lipopolysaccharide-induced intestinal injury in mice via alpha 2 adrenoceptor-independent mechanisms. *Acta Pharmacol Sin* 2011;32:1364–72.
- [10] Williams JM, Duckworth CA, Watson AJ, Frey MR, Miguel JC, Burkitt MD, et al. A mouse model of pathological small intestinal epithelial cell apoptosis and shedding induced by systemic administration of lipopolysaccharide. *Dis Model Mech* 2013;6:1388–99.
- [11] Turner JR. Molecular basis of epithelial barrier regulation—from basic mechanisms to clinical application. *Am J Pathol* 2006;169:1901–9.
- [12] Doss M, White MR, Teclé T, Hartshorn KL. Human defensins and LL-37 in mucosal immunity. *J Leukoc Biol* 2010;87:79–92.
- [13] Lai YP, Gallo RL. AMPed up immunity: how antimicrobial peptides have multiple roles in immune defense. *Trends Immunol* 2009;30:131–41.
- [14] Gallo RL, Kim KJ, Bernfield M, Kozak CA, Zanetti M, Merluzzi L, et al. Identification of CRAMP, a cathelin-related antimicrobial peptide expressed in the embryonic and adult mouse. *J Biol Chem* 1997;272:13088–93.
- [15] Mookherjee N, Brown KL, Bowdish DME, Doria S, Falsafi R, Hokamp K, et al. Modulation of the TLR-mediated inflammatory response by the endogenous human host defense peptide LL-37. *J Immunol* 2006;176:2455–64.
- [16] Nell MJ, Tjallingii GS, Wafelman AR, Verrijck R, Hiemstra PS, Drijfhout JW, et al. Development of novel LL-37 derived antimicrobial peptides with LPS and LTA neutralizing and antimicrobial activities for therapeutic application. *Peptides* 2006;27:649–60.
- [17] Scott MG, Davidson DJ, Gold MR, Bowdish D, Hancock REW. The human antimicrobial peptide LL-37 is a multifunctional modulator of innate immune responses. *J Immunol* 2002;169:3883–91.
- [18] Schaubert J, Rieger D, Weiler F, Wehkamp J, Eck M, Fellerermann K, et al. Heterogeneous expression of human cathelicidin hCAP18/LL-37 in inflammatory bowel diseases. *Eur J Gastroenterol Hepatol* 2006;18:615–21.
- [19] Ye Y, Xing H, Chen X. Anti-inflammatory and analgesic activities of the hydrolyzed sasanquasaponins from the defatted seeds of *Camellia oleifera*. *Arch Pharm Res* 2013;36:941–51.
- [20] Tai EKK, Wu WKK, Wong HPS, Lam EKY, Yu L, Cho CH. A new role for cathelicidin in ulcerative colitis in mice. *Exp Biol Med* 2007;232:799–808.
- [21] Wang YP, Zhang ZY, Chen LL, Guang HJ, Li Z, Yang HL, et al. Cathelicidin-BF, a snake cathelicidin-derived antimicrobial peptide, could be an excellent therapeutic agent for *Acne vulgaris*. *PLoS ONE* 2011;6.
- [22] Wang Y, Hong J, Liu X, Yang H, Liu R, Wu J, et al. Snake cathelicidin from *Bungarus fasciatus* is a potent peptide antibiotics. *PLoS ONE* 2008;3:e3217.
- [23] Schneider CA, Rasband WS, Eliceiri KW. NIH Image to ImageJ: 25 years of image analysis. *Nat Methods* 2012;9:671–5.
- [24] Chiu CJ, McArdle AH, Brown R, Scott HJ, Gurd FN. Intestinal mucosal lesion in low-flow states 1. a morphological, hemodynamic, and metabolic reappraisal. *Arch Surg* 1970;101:478–8.
- [25] Gu LL, Li N, Gong JF, Li QR, Zhu WM, Li JS. Berberine ameliorates intestinal epithelial tight-junction damage and down-regulates myosin light chain kinase pathways in a mouse model of endotoxemia. *J Infect Dis* 2011;203:1602–12.
- [26] Kiesslich R, Duckworth CA, Moussata D, Gloeckner A, Lim LG, Goetz M, et al. Local barrier dysfunction identified by confocal laser endomicroscopy predicts relapse in inflammatory bowel disease. *Gut* 2012;61:1146–53.
- [27] Copeland S, Warren HS, Lowry SF, Calvano SE, Remick D, Inflammation Host R. Acute inflammatory response to endotoxin in mice and humans. *Clin Diagn Lab Immunol* 2005;12:60–7.
- [28] Abreu MT. Toll-like receptor signalling in the intestinal epithelium: how bacterial recognition shapes intestinal function. *Nat Rev Immunol* 2010;10:131–43.
- [29] Beutler B, Greenwald D, Hulmes JD, Chang M, Pan YCE, Mathison J, et al. Identity of tumor necrosis factor and the macrophage-secreted factor cachectin. *Nature* 1985;316:552–4.
- [30] Chin AC, Flynn AN, Fedwick JP, Buret AG. The role of caspase-3 in lipopolysaccharide-mediated disruption of intestinal epithelial tight junctions. *Can J Physiol Pharmacol* 2006;84:1043–50.
- [31] Park EJ, Thomson ABR, Clandinin MT. Protection of intestinal occludin tight junction protein by dietary gangliosides in lipopolysaccharide-induced acute inflammation. *J Pediatr Gastroenterol Nutr* 2010;50:321–8.
- [32] Al-Sadi R, Khatib K, Guo SH, Ye DM, Youssef M, Ma T. Occludin regulates macromolecule flux across the intestinal epithelial tight junction barrier. *Am J Physiol Gastrointest Liver Physiol* 2011;300:G1054–64.
- [33] Ma TY, Boivin MA, Ye DM, Pedram A, Said HM. Mechanism of TNF-alpha modulation of Caco-2 intestinal epithelial tight junction barrier: role of myosin light-chain kinase protein expression. *Am J Physiol Gastrointest Liver Physiol* 2005;288:G422–30.
- [34] Al-Sadi R, Ye DM, Dokladny K, Ma TY. Mechanism of IL-1 beta-induced increase in intestinal epithelial tight junction permeability. *J Immunol* 2008;180:5653–61.
- [35] Ranaivo HR, Carusio N, Wangenstein R, Ohlmann P, Loichot C, Tesse A, et al. Protection against endotoxic shock as a consequence of reduced nitrosative stress in MLCK210-null mice. *Am J Pathol* 2007;170:439–46.